Coupling of Underground Pipelines and Slowly Moving Landslides by BEM Analysis

A. Mandolini[1], V. Minutolo[1], E. Ruocco[1]

Abstract: Many sloping areas in the world are affected by slow movements. If they are occupied by settlements or are crossed by roads, pipelines or other infrastructures, a correct evaluation of future displacements is crucial for land management and sometimes for men safety. It is widely recognized that rainfall is the main triggering factor, producing an intermittent and delayed recharge of the groundwater; as a consequence, the displacement rate is cyclic, following a seasonal trend. In Italy this problem is particularly relevant since many exploited sloping areas are affected by slowly moving landslides that interact with man-made works. In present paper a BEM procedure is proposed and a case study is analyzed concerning underground pipelines in moving landslides.

1 Introduction

Landslides, like other natural events as floods, earthquakes, avalanches and volcanic eruptions, are natural hazards causing large economic and human losses. Often such phenomena are translational and involve fine-grained soils inducing continuous damages to roads, railways, pipelines for gas or hydrocarbon transportation, industrial and civil settlement, etc.

The costs required for reparation or deriving from failures of service are very high. Furthermore, sometimes human lives are exposed to a high-risk also in the case of very slow slope movements (e.g. for sudden failure of a pipeline for high-pressure gas transportation).

The selection of the exploitation criteria of unstable slowly moving slopes is always characterized by large uncertainties. In fact, it is often not possible to carry out drastic slope stabilization works and therefore it becomes necessary to adopt advanced and sophisticated management criteria. In such cases the acceptable and tolerable risks from landsliding have to be defined. This stimulates the selection of strategies based on criteria belong-

ing to the Decision-Making Analysis. In particular, the case of slowly moving landslides is a peculiar one specially suited for integrating the classical analysis methods with procedures capable of usefully exploiting data coming from monitoring and experience, the well-known observational method. In fact, the movement's slowness and the availability of long time data allow to define the best management strategies and to continuously refine the methods of analysis, the control procedures and the design criteria of stabilization works.

In this context, here is presented a case of a pipeline crossing a slowly moving landslide under monitoring in the last years. A numerical procedure was implemented in order to: i) predict the evolution of the phenomena in terms of induced stress into the pipeline coming from the displacement field of the surrounding soil, ii) make available a general code that, from a typical set of slope displacement data, is able to analyze the stress-strain behaviour of similar structures, but in different conditions from those regarding the examined case.

In the following, after a brief description of the site and of the collected data from monitoring, a detailed overview of the adopted numerical approach will be given. Finally, a comparison between experimental data and numerical prediction will be shown and some conclusion will be drawn.

2 Site description and experimental observation

The examined landslide is a typical earthflow in a final stage of evolution with morphological features (main scarp and lateral boundaries) not anymore clearly recognizable (Figure 1). Its length may be estimated in about 1000 m; the average slope is $9.5°$. A small stream flows at the slope toe, adding the contribution of some erosion to the other factors governing the landslide movement.

The earthflow involves highly plastic intensely fissured clay shales; the main landslide body is constituted by rather inhomogeneous softened materials.

[1] Department of Civil Engineering, Second University of Naples, Via Roma 29, 81031 Aversa, Ce, Italy.
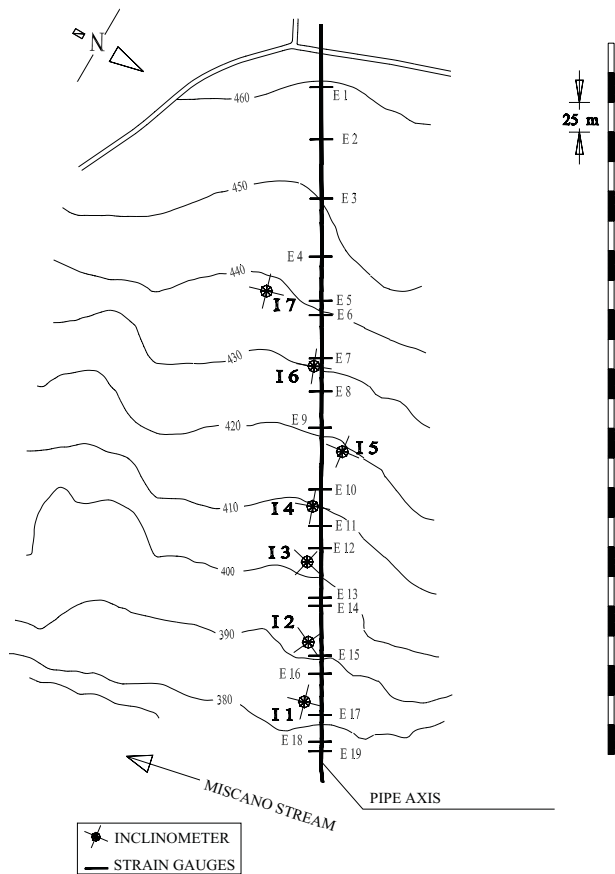
Figure 1 : Investigated slope: instrumentation and pipeline location

Figure 2 : Landslide body as revealed through inclinometer measurements and boreholes

The landslide is crossed longitudinally by a gas pipeline (d = 0.6 m), located at a depth of about 2 m (Figure 1). The slope is instrumented with 7 inclinometers and 20 piezometers, installed at different times close to the pipeline. An automatic rainfall gauge was installed on January, 1995. Further data on the rainfall height between 1985 and 1995 have been provided by official files collected by the pluviometer station of Ginestra degli Schiavoni, located in the same hydrographic basin.

In October, 1995, the soil around the pipeline was temporarily excavated in order to instrument the pipeline with vibrating wire extensometers, for a total number of 45 (15 instrumented sections, each one equipped with 3 extensometers in symmetrical position). The zero readings were taken more than one month later.

Figure 2 shows a slope longitudinal section, which is referred to the elevation above sea level, as revealed by the inclinometer displacement profiles and from the thickness of the remoulded soil during the site investigations. It can be seen that the slip surface is quite shallow (3÷4 m) in the upper part of the slope, and deepens (14÷15 m) at the toe (accumulation zone).

Figure 3 summarizes the main results of monitoring with reference to only landslide displacement and axial force as deduced from strain measurements.

It can be seen that the displacement of the landslide is different along the landslide body itself, ranging between 8.2 and 94.4 mm in the upper part of the slope and between 57.6 and 107.3 in the lower part (accumulation zone); such values are referred to a time period of almost 40 months, giving a maximum local rate of displacement of 4.2 mm/month (I3) and a minimum local rate of displacement of 0.2 mm/month (I4).

In the upper part of the Figure 3 are reported both the distribution of the displacement along the landslide and of the axial force along the pipeline as measured on February, 23, 1999. Starting from the upper part of the slope, it can be seen that up to almost 370 m the pipeline is under an increasing axial force, meaning that the soil is acting onto the pipeline with "negative" traction; on the contrary, from 370 m to 500 m the axial force decreases and thus the tractions become "positive". In the remaining 100 m, no decrease of force is measured, that means no interaction between soil and pipeline occurs.
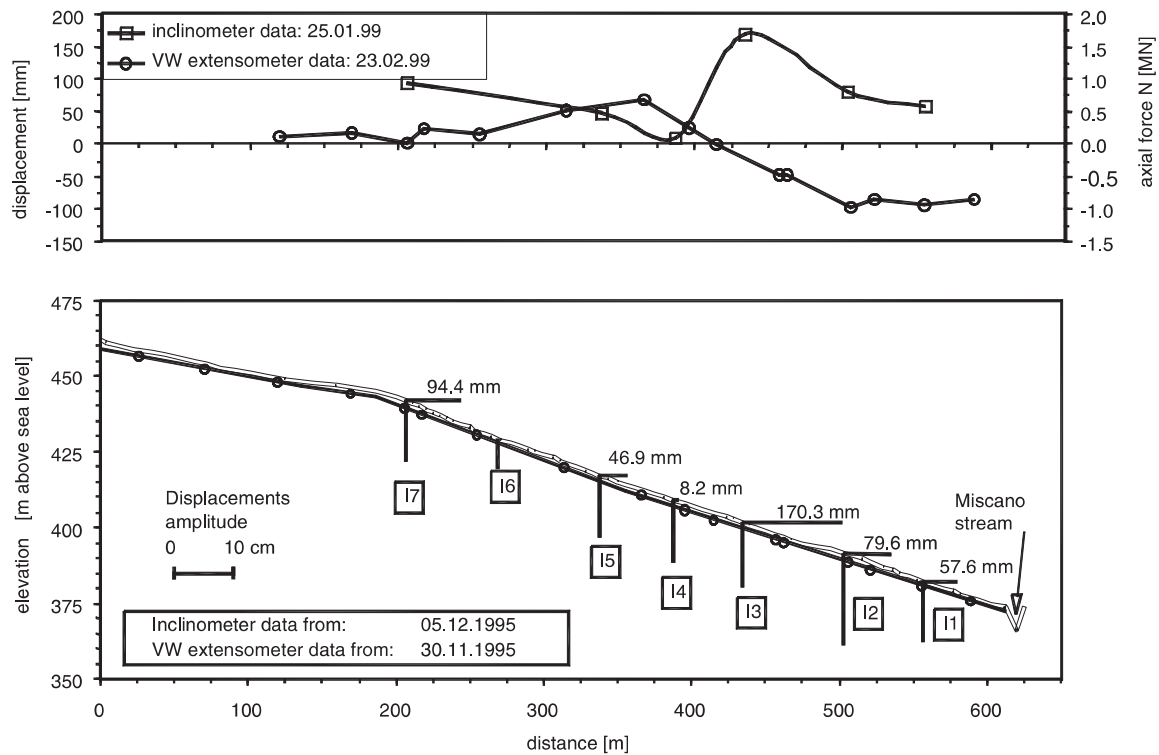
Figure 3 : Relevant displacements, axial force on pipeline and sliding displacements of soil

3   Models of the analysis

The prediction of the limit displacement, leading to pipe collapse, with respect to the interaction with the sliding soil, have been reached in Rajani and Morgenstern (1994), Rajani, Robertson, and Morgenstern (1995), Rizkalla and McImtye (1991); in particular Rajani, Robertson, and Morgenstern (1995) and Rizkalla and McImtye (1991) deals with a simplified procedure characterized by the implementation of a spring model for the soil. They derived the knowledge of pipe maximum stress by the mean displacement of soil mass that is supposed to have rigid body motion. This approach gives a simple evaluation of the soil displacement amplitude yielding to pipeline failure, but does not take into account three dimensional constitutive model of the soil and gives no information about pipe and soil stress distribution.

The treatment of experimental data needs to introduce some simplifications namely, landslide has large transversal dimension in comparison to the diameter of the pipe and can be assumed to have infinite size. The value of the displacement along meridian curves of landslide can be assumed as a constant with respect to transversal direction.

Boundary Integral Equation Method (BIEM) is implemented to formulate the soil model. It was seen Aliabadi and Martìn (1998) that BIEM has effective advantages in solving soil structure interaction because, among others, it allows for the discretisation of small parts of the soil boundary where contact takes place. In a more general sense, the Boundary Element Method is a way of solving the contact problem which, compared with other methods of numerical analysis, seems to be a feasible tool especially because of: the relevant parameters for the friction contact models, particularly in Coulomb model, are direct independent variables of the BEM, i.e. the displacements and the tractions associated with outward normal at boundary point; the non linear features of the problem (size of the contact zone and presence of relative tangential displacements) are associated with boundary points and appear directly in the boundary element for-
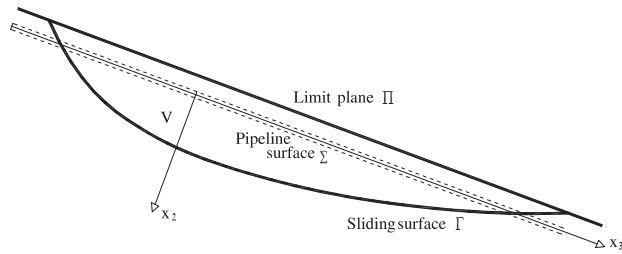
Figure 4 : Soil Volume and Boundary Model

mulation.

Numerical procedures are derived by the simplifications previously described that are gained to the possibility to get data files restricted to meridian curve of the sliding surface. In following sections general models for the soil and the pipe are presented; subsequently the models are coupled and results are compared to the experimental data coming from the Miscano site. In order to obtain the desired coupling between three-dimensional soil model and one-dimensional beam a suitable condensation of the degrees of freedom has been done.

4   Soil equations

In figure 4 the soil volume is represented; it consists of a three dimensional space subset, V, bounded by the sliding surface Γ, by the cylindrical soil pipe interface Σ and by the part Π of limit plane intercepted by Γ. The global Cartesian orthogonal frame has axis x_3 coincident with pipe axis, x_2 belonging to the vertical plane passing through x_3 and x_1 resulting from right hand law.

The reciprocity Betti's theorem, formulated between the body V subjected to boundary tractions **t** and displacements **u,** and Kelvin's elastic state, originates the following Boundary Integral Equation (BIE):

$$\mathbf{C}(\xi)\,\mathbf{u}(\xi) = \int_{\partial V} \mathbf{G}(\mathbf{x},\xi)\,\mathbf{t}(\mathbf{x})\,d\mathbf{x} - \int_{\partial V} F(\mathbf{x},\xi)\,u(\mathbf{x})\,d\mathbf{x}$$
$$+ \int_V \mathbf{G}(\mathbf{x},\xi)\,\mathbf{b}(\mathbf{x})\,d\mathbf{x} \qquad (1)$$

In Eq.1 the Kelvin's solution, i.e. fundamental solution, has the explicit expression (see for example Hartmann

(1989)):

$$\mathbf{G}(\mathbf{x},\xi) = \frac{1}{16\pi\mu(1-\nu)\,r}\left[(3-4\nu)\,\mathbf{I} + \nabla r \otimes \nabla r\right] \qquad (2)$$

$$\mathbf{F}(\mathbf{x},\xi) = \frac{1}{8\pi(1-\nu)\,r}\{(1-2\nu)\,(\mathbf{n}\otimes\nabla r - \nabla r\otimes\mathbf{n})$$
$$+ (\nabla r \cdot \mathbf{n})\left[(1-2\nu)\,\mathbf{I} + 3\nabla r\otimes\nabla r\right]\} \qquad (3)$$

where r is the magnitude of the position vector of integration point **x** with respect to the variable source point ξ, ν and μ are soil elastic constants (i.e. Poisson ratio and shear modulus).

The discretization of Eq. 1 is performed by the introduction of surface elements; in particular the external boundary, i.e. the surface $\Gamma \cup \Pi$ of sliding soil volume is modeled by means of infinite strips having their longitudinal direction parallel to x_1 axis. The transversal variability of shape function in each strip is assumed to be quadratic, moreover constant functions are selected to model longitudinal behaviour of displacements and tractions. A set of local coordinate (η, ζ) is introduced (see figure 5).

The soil-pipe interface, surface Σ, is divided into cylindrical elements of length λ_k and radius R; a cylindrical local coordinate system is introduced, consisting of angular coordinate φ and axial coordinate τ. The origin is set at the middle point P_k of the element axis. Subsequent analysis is carried out assuming vanishing bending effects; this hypothesis implies that displacements and tractions can be mapped by means of constant shape functions with respect to φ.

Eq. 1 is therefore transformed accordingly to the decomposition of integrals over boundary elements. It results in the following form where, for sake of compactness, the body forces have been neglected:

$$\mathbf{C}(\xi)\,\mathbf{u}(\xi) = \sum_{NE}\left\{\mathbf{t}^e\int_{-1}^{1}N(\eta)\,J(\eta)\int_{-\infty}^{\infty}G(x(\eta,\zeta),\xi)\,d\zeta d\eta\right.$$

$$\left. +\mathbf{u}^e\int_{-1}^{1}N(\eta)\,J(\eta)\int_{-\infty}^{\infty}F(x(\eta,\zeta),\xi)\,d\zeta d\eta\right\}$$

$$+\sum_{NI}\left\{\frac{\lambda_k}{2}\mathbf{t}_\Sigma\int_{-1}^{1}\int_{0}^{2\pi}G(x(\varphi,\tau),\xi)\,Rd\varphi d\tau\right.$$

$$\left. +\frac{\lambda_k}{2}\mathbf{u}_\Sigma\int_{-1}^{1}\int_{0}^{2\pi}F(x(\varphi,\tau),\xi)\,Rd\varphi d\tau\right\} \qquad (4)$$

$$N^{P_1}(\eta) = \frac{1}{2}\eta(1-\eta)$$

$$N^{P_2}(\eta) = (\eta+1)(1-\eta)$$

$$N^{P_3}(\eta) = \frac{1}{2}\eta(\eta+1)$$

$$-1 < \eta < 1$$

$$-\infty < \zeta < \infty$$

$$x_\alpha^P(\eta,\zeta) = N^{P_i}(\eta)x_\alpha^{P_i}; \quad \alpha \in \{1,3\}$$

$$x_2^P(\eta,\zeta) = \zeta; \qquad i \in \{1,2,3\}$$

$$u_j(\eta,\zeta) = N^{P_i}(\eta)u_j^{P_i};$$

$$t_j(\eta,\zeta) = N^{P_i}(\eta)t_j^{P_i}; \quad i,j \in \{1,2,3\}$$
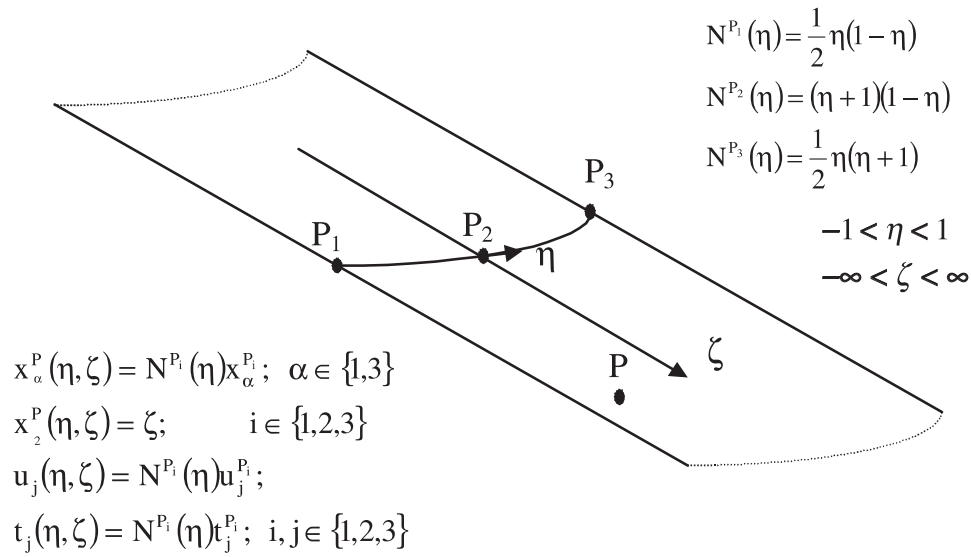
Figure 5 : Shape functions and geometry representation on external Boundary Elements

The right hand side variables in Eq. 4 are the nodal values of unknown fields **t** and **u**. Left hand side contains unknown value of displacement field at source point ξ. It has to be noted that no collocation has been done to obtain Eq. 4. The first sum in Eq. 4 is performed on the number *NE* of elements belonging to $\Gamma \cup \Pi$, i.e. the external boundary. $J(\eta)$ represents the Jacobean of the coordinate transformation. The second sum in Eq. 4 is performed on the number *NI* of elements belonging to Σ; the Jacobean, in this case, has the value $\lambda_k/2$.

The vectors $\mathbf{t}^e$ and $\mathbf{u}^e$ are the nodal values of the traction and of the displacement fields on the external boundary and are partitioned into two sub-vectors containing the nodal values of tractions and displacements belonging to the limit plane and to the sliding surface respectively:

$$\mathbf{t}^e = \begin{bmatrix} \mathbf{t}_\Pi \\ \mathbf{t}_\Gamma \end{bmatrix}$$

$$\mathbf{u}^e = \begin{bmatrix} \mathbf{u}_\Pi \\ \mathbf{u}_\Gamma \end{bmatrix}$$

Once the equation has been collocated on boundary points that belongs to the external boundary it is possible to obtain 2*NE* equations involving nodal variables: Eq. 4 is modified by means of analytical integration over $]-\infty, \infty[$ of the right hand side which reduces the fundamental solution terms contained in the first two integrals

to 2D-like kernels Telles (1983). These functions have the same expression of standard 2D fundamental solution provided to reverse the role played by source point ξ and integration variable **x**. The first two integrals reduces to 2D standard problem that does not depend on the coordinate x_1.

The two integrals on cylindrical domain, Σ, with respect to the variable φ, behaves as axisymmetric kernels provided to exchange the meaning of source point with integration point, Karmanidis (1975); even in the case of integration over cylindrical boundary it is possible to assume plane behaviour of the system.

The above mentioned considerations suggest that the analysis can be limited to 2D geometry, displacements and tractions; moreover the singularity of cylindrical kernels with respect to the in plane coordinates is of the same logarithmic type of the singularity of 2D-like kernels that arise from the integration on the external boundary. The same attention as in the case of plane solution has been devoted to cylindrical integrals and the same numerical quadrature formulas has been adopted.

Particular attention is needed in order to collocate Eq. 4 on points of Σ. The left hand side of Eq. 4 represents the displacement of a point on the cylindrical boundary Σ in terms of tractions and displacements of the whole boundary V. Due to the shape functions introduced in

the right hand side of the boundary equation and to the integration performed with respect to out of plane variables, it appears evident that nodal variables $\mathbf{u}_\Sigma$ and $\mathbf{t}_\Sigma$ represent the mean value of displacement and traction on the directrix circumference of each element at point P_k. To obtain the same number of equations and unknowns it is necessary to collocate Eq. 1 using a unit ring load, applied at the point P_k. The ring load has unity value that do not vary with respect to the local angular coordinate. The angular variable corresponding to source point has been called θ. Performing the integration of boundary equations with respect to θ, the collocated equation on Σ will be transformed accordingly to the following relationship:

$$\int_0^{2\pi} \frac{1}{2} \mathbf{I} \mathbf{u}(\theta,\lambda) R d\theta = \pi R \mathbf{I} \mathbf{u}_\Sigma =$$

$$\int_0^{2\pi} \left\{ \sum_{NE} \left[\mathbf{t}^e \int_{-1}^1 \mathbf{N}(\eta) J(\eta) \int_{-\infty}^\infty \mathbf{G}(\mathbf{x}(\eta,\zeta),\xi(\theta,\lambda)) \, d\tau d\zeta \right. \right.$$

$$\left. + \mathbf{u}^e \int_{-1}^1 N(\eta) J(\eta) \int_{-\infty}^\infty \mathbf{F}(\mathbf{x}(\eta,\zeta),\xi(\theta,\lambda)) \, d\tau d\zeta \right]$$

$$+ \sum_{NI} \frac{\lambda_i}{2} \mathbf{t}_\Sigma \int_{-1}^1 \int_0^{2\pi} \mathbf{G}(\mathbf{x}(\varphi,\tau),\xi(\theta,\lambda)) R d\varphi d\tau$$

$$\left. + \frac{\lambda_i}{2} \mathbf{u}_\Sigma \int_{-1}^1 \int_0^{2\pi} \mathbf{F}(\mathbf{x}(\varphi,\tau),\xi(\theta,\lambda)) R d\varphi d\tau \right\} R d\theta \qquad (5)$$

Left-hand side of Eq. 5 contains the mean value of displacement $\mathbf{u}$, giving a suitable matching of variables on right hand side. Finally the following matrix form is obtained:

$$\begin{bmatrix} \mathbf{H}_{\Pi\Pi} & \mathbf{H}_{\Pi\Gamma} & \mathbf{H}_{\Pi\Sigma} \\ \mathbf{H}_{\Gamma\Pi} & \mathbf{H}_{\Gamma\Gamma} & \mathbf{H}_{\Gamma\Sigma} \\ \mathbf{H}_{\Sigma\Pi} & \mathbf{H}_{\Sigma\Gamma} & \mathbf{H}_{\Sigma\Sigma} \end{bmatrix} \begin{bmatrix} \mathbf{u}_\Pi \\ \mathbf{u}_\Gamma \\ \mathbf{u}_\Sigma \end{bmatrix} =$$

$$\begin{bmatrix} \mathbf{G}_{\Pi\Pi} & \mathbf{G}_{\Pi\Gamma} & \mathbf{G}_{\Pi\Sigma} \\ \mathbf{G}_{\Gamma\Pi} & \mathbf{G}_{\Gamma\Gamma} & \mathbf{G}_{\Gamma\Sigma} \\ \mathbf{G}_{\Sigma\Pi} & \mathbf{G}_{\Sigma\Gamma} & \mathbf{G}_{\Sigma\Sigma} \end{bmatrix} \begin{bmatrix} \mathbf{t}_\Pi \\ \mathbf{t}_\Gamma \\ \mathbf{t}_\Sigma \end{bmatrix} \qquad (6)$$

The subscripts in Eq. 6 point out the collocation and the integration points. Off diagonal terms of matrices are calculated by means of standard Gauss' quadrature. Diagonal sub-matrices of order two, $\mathbf{H}_{\alpha\beta}$, are evaluated by means of the rigid body condition.

Due to the fact that the integrand functions to obtain $H_{\Sigma\Sigma}$ are defined in rectangular coordinates, the rigid body condition can be used with respect to axisymmetric-like kernels too. It has to be noted that the sum of row submatrices of order two of $H_{\Sigma\Pi}$ and $H_{\Sigma\Gamma}$ vanishes because matrix $H_{\Sigma\Sigma}$ represents the opposite of the matrix corresponding to the application of BEM to the volume of the pipe supposed fulfilled by soil material. Thus the diagonal submatrices of order two belonging to $H_{\Sigma\Sigma}$ can be obtained by the opposite of the sum of the off diagonal terms of $H_{\Sigma\Sigma}$.

In the calculation of the elements of the **G** matrix, a logarithmic quadrature formula is used for singular terms, a standard Gauss formula has been used for the regular terms.

5 Pipe model

In the following it has been supposed that the beam undergoes to bending along a prefixed direction. Displacements of pipe points are described accordingly to Bernoulli hypothesis by following functions with respect to local orthogonal frame (O,x,y,z) (see Figure 6) where y axis belongs to bending plane:

$$u_x = u_x(0,0,z) = u_0(z) \qquad (7)$$

$$u_y = u_y(0,0,z) = v_0(z) \qquad (8)$$

$$u_z = u_z(0,0,z) - v_{0,z}y = w_0(z) - v_{0,z}y \qquad (9)$$

u_0, v_0, w_0 represent the displacements of the line of centroids of the beam which is chosen as the z axis; $v_{0,z}$ is the derivative of v_0 with respect to z representing the slope of the deformed axis of the structure. Basing on the fact that pipeline is embedded in landsliding soil mass having axial direction parallel to maximum slope and supposing that bending stiffness of the pipe can be neglected with respect to axial stiffness, the attention has been focused on the equilibrium in axial direction:

$$EAw_0^{II} = -q_z \qquad (10)$$

where EA is the axial stiffness of the beam. The displacement field has vanishing u_x and u_y components, whereas the axial component u_z is constant with respect to y.

Obviously, the Bernoulli model does not take into account actual distribution of axial load q_z with respect to the circumference of beam cross section.

Eq. 10 is discretised by finite element method. Rod finite elements were selected, with cross sectional area A,
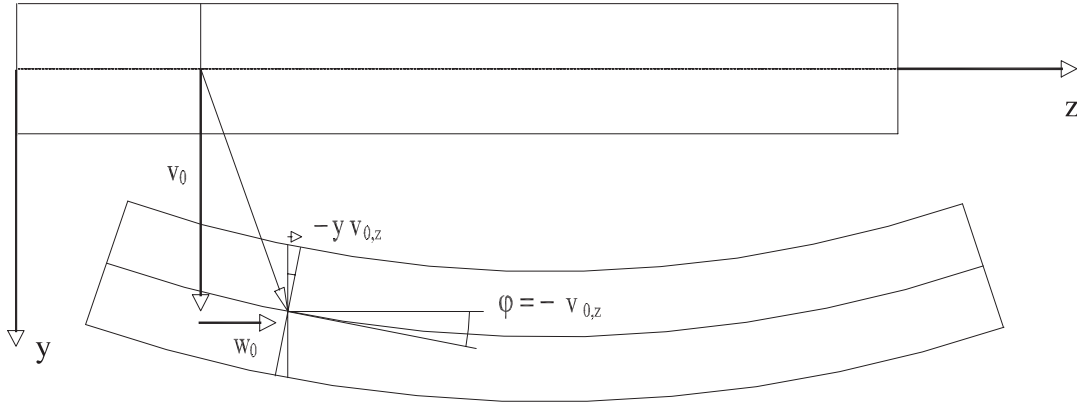
Figure 6 : Beam local coordinate system and displacements

Young's modulus E, length λ_k. Stiffness matrix of the elements spans axial and transversal components of nodal points displacement, $\mathbf{u}_k^p$, in axial and transversal components of nodal forces, $\mathbf{f}_k$. The resulting equation is:

$$\mathbf{f}_k = \mathbf{K}_k \mathbf{u}_k^p + \mathbf{f}_k^0 \tag{11}$$

where:

$$\mathbf{K}_k = \begin{bmatrix} EA/\lambda_k & 0 & EA/\lambda_k & 0 \\ 0 & 0 & 0 & 0 \\ EA/\lambda_k & 0 & EA/\lambda_k & 0 \\ 0 & 0 & 0 & 0 \end{bmatrix} \tag{12}$$

$$\mathbf{u}_k^p = \begin{bmatrix} u_y^i \\ u_z^i \\ u_y^j \\ u_z^j \end{bmatrix} \qquad \mathbf{f}_k^0 = \begin{bmatrix} f_y^{0i} \\ f_z^{0i} \\ f_y^{0j} \\ f_z^{0j} \end{bmatrix} \qquad \mathbf{f}_k = \begin{bmatrix} f_y^i \\ f_z^i \\ f_y^j \\ f_z^j \end{bmatrix}$$

$\mathbf{f}_k^0$ represents the fixed end forces produced by the applied axial load; it can be evaluated by assuming linear variation of load with the abscissa z.

By collecting the nodal values of axial load distribution on k^{th} element into the vector $\mathbf{q}_k = \begin{bmatrix} q_y^i, q_z^i, q_y^j, q_z^j \end{bmatrix}^T$, a linear operator $\mathbf{L}_k$, transforming $\mathbf{q}_k$ into $\mathbf{f}_k^0$, can be introduced and matrix form of the application defined as follows:

$$\begin{bmatrix} f_y^{0i} \\ f_z^{0i} \\ f_y^{0j} \\ f_z^{0j} \end{bmatrix} = \begin{bmatrix} \lambda_k/3 & 0 & \lambda_k/6 & 0 \\ 0 & 0 & 0 & 0 \\ \lambda_k/6 & 0 & \lambda_k/3 & 0 \\ 0 & 0 & 0 & 0 \end{bmatrix} \begin{bmatrix} q_y^i \\ q_z^i \\ q_y^j \\ q_z^j \end{bmatrix} \tag{13}$$

Eq. 11, 12 and 13 can be assembled in a standard way to define the overall equilibrium equation of the structure:

$$\mathbf{K}\mathbf{u}^p + \mathbf{L}\mathbf{q} = \mathbf{0} \tag{14}$$

where $\mathbf{K}$ and $\mathbf{L}$ represent the matrices resulting from the assemblage of $\mathbf{K}_k$ and $\mathbf{L}_k$. Eq. 14 is the final relationship between axial and transversal displacement field of the beam axis and resultant per unit length of pipe axis, q_z, of boundary tractions acting on the lateral surface of the beam itself.

6 Coupling equations

Soil volume, as previously described, is subjected to interface tractions on the sliding surface that derive from the contact between stable soil and moving soil mass. Moreover tractions take place on soil pipe interface.

Pipe model, as introduced previously, allows for the analysis of the pipe response to axial loads applied to the circumference of cross sections. More general coupling equations, that take into account the bending effects, can be obtained by the procedure outlined in Guarracino, Minutolo, and Nunziante (1992). Moreover the aforementioned equations have to be coupled with boundary conditions involving end displacements and reactions on the pipe; both prescribed displacements values or elastic springs can be introduced, giving a modification of some diagonal term of $\mathbf{K}$ matrix as in standard FEM analysis.

The coupling between soil and pipe model has been reached by assuming the following relationship between
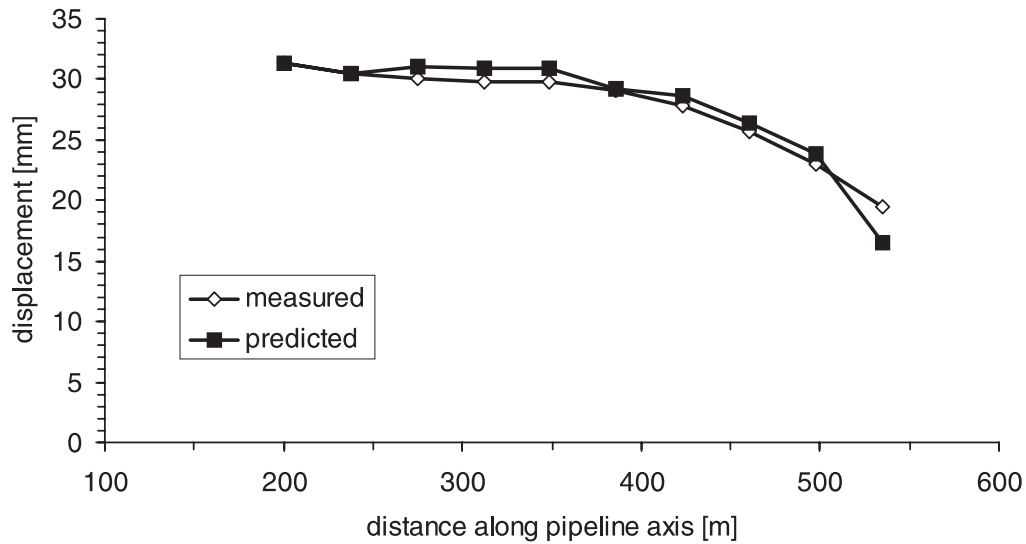
Figure 7 : Comparison of displacements calculated by BEM soil model and by beam model from measured strain

tractions which are present in Eq. 6 and beam axial nodal load involved in Eq. 14:

$$\mathbf{t}_\Sigma = -\frac{\mathbf{q}}{2\pi R} \qquad (15)$$

In the case of no sliding between pipe and soil, as confirmed by the collected experimental evidence, the displacements $\mathbf{u}^p$ in Eq. 14 are set equal to the displacements $\mathbf{u}_\Sigma$ in Eq. 6.

The coupling of Eq. 6 with Eq. 14 results in the following set of equations that describes the pipe soil interaction in the case of long pipes without sliding effects:

$$\begin{bmatrix} \mathbf{H}_{\Pi\Pi} & \mathbf{H}_{\Pi\Sigma} & -\mathbf{G}_{\Pi\Gamma} & -\mathbf{G}_{\Pi\Sigma} \\ \mathbf{H}_{\Gamma\Pi} & \mathbf{H}_{\Gamma\Sigma} & -\mathbf{G}_{\Gamma\Gamma} & -\mathbf{G}_{\Gamma\Sigma} \\ \mathbf{H}_{\Sigma\Pi} & \mathbf{H}_{\Sigma\Sigma} & -\mathbf{G}_{\Sigma\Gamma} & -\mathbf{G}_{\Sigma\Sigma} \\ & \mathbf{K} & & \mathbf{L} \end{bmatrix} \begin{bmatrix} \mathbf{u}_\Pi \\ \mathbf{u}_\Sigma \\ \mathbf{t}_\Gamma \\ \mathbf{t}_\Sigma \end{bmatrix} =$$

$$\begin{bmatrix} \mathbf{H}_{\Pi\Gamma} & \mathbf{G}_{\Pi\Pi} \\ \mathbf{H}_{\Gamma\Gamma} & \mathbf{G}_{\Gamma\Pi} \\ \mathbf{H}_{\Sigma\Gamma} & \mathbf{G}_{\Sigma\Pi} \\ \mathbf{0} & \mathbf{0} \end{bmatrix} \begin{bmatrix} \mathbf{u}_\Gamma \\ \mathbf{t}_\Pi \end{bmatrix} \qquad (16)$$

The presence of sliding between pipe and soil can be analysed by means of Eq. 16 coupling it with yield criterion and performing an incremental analysis as in Aliabadi and Martìn (1998).

7 Numerical examples and comparison with experimental results

The proposed procedure has been applied to the Miscano pipeline. The measured soil displacements on sliding surface, as reported in figure 3, have been applied as boundary conditions. The vector $\mathbf{u}_\Gamma$ in Eq. 6 is thus prescribed; moreover, vanishing $\mathbf{t}_\Pi$ are assumed. Eq. 6 is solved in terms of unknown variables $\mathbf{u}_\Pi$, $\mathbf{u}_\Sigma$, $\mathbf{t}_\Gamma$, $\mathbf{t}_\Sigma$. The resulting displacements on pipeline axis, $\mathbf{u}_\Sigma$, are shown in figure 7. In the same figure the displacements calculated by means of integration of strain measurements on pipeline surface have been reported. The comparison between the two curves is rather satisfactory. It have to be mentioned that the integrated displacement has an unknown initial value; therefore the comparison has been made by imposing the coincidence of first point displacement. The calculated tractions on soil-pipeline surface have a maximum axial value of $113.59\,kgm^{-2}$, to be combined with a minimum radial pressure is 1440.0 kgm^{-2}, giving a stress point within any yielding surface as, for instance, that derived by the Coulomb strenght criterion by assuming an internal soil friction angle equal to the minimum value measured by laboratory and site tests $(\phi = 25°)$. This finding confirms the goodness of the adopted approach (no sliding between soil and pipe), allowing to use it in an incremental analysis aimed to the

definition of the collapse condition for the pipe subjected to increasing soil movements due to landsliding process.

8 Conclusions

The analysis described in the present paper allows to evaluate the response of pipelines embedded in soil mass undergoing to displacement field. The Boundary Integral Equation Method seems to be a suitable approach for the analysis of soil pipe interaction. In particular, when field experimental data are available, the proposed approach can be used for pipeline management. Infact, by calibrating all the relevant parameters for the model on the basis of the already collected data, it become possible to implement an iterative procedure aimed to the prediction of future pipeline behaviour during its timelife as a consequence of soil displacements

It has to be stressed that the research activity is at the preliminary stage. Further experimental data concerning with different soil types, dispalcement fields and pipeline geometry and characteristics have to be collected, as well as further analysis have to be carried out before any conclusion could be drawn.

References

Aliabadi, M. H.; Martìn, D. (1998): Boundary element analysis of two-dimensional elastoplastic contact problems. *Eng. Anal. with Boundary Element Method*, vol. 21, pp. 349–360.

Guarracino, F.; Minutolo, V.; Nunziante, L. (1992): A simple analysis of soil structures interaction by BEM-FEM coupling. *Eng. Anal. with Boundary Element Method*, vol. 10, pp. 283–289.

Hartmann, F. (1989): *Introduction to Boundary Elements*. Springer Verlag.

Karmanidis, T. (1975): A numerical solution for axially symmetrical elasticity problems. *International Journal of Solids and Structures*, vol. 11, pp. 493–500.

Rajani, B.; Morgenstern, N. R. (1994): Comparison of predicted and observed response of pipeline to differential frost heave. *Can. Geotech. J.*, vol. 31.

Rajani, B.; Robertson, P. K.; Morgenstern, N. R. (1995): Simplified design methods for pipelines subjected to transverse and longitudinal soil movements. *Can. Geotech. J.*, vol. 32.

Rizkalla, M.; McImtye, M. B. (1991): A special pipeline design for unstable slopes. *ASME Proc.*, vol. 34.

Telles, J. F. C. (1983): *The Boundary Element Method Applied to Inelastic Problem*. Springer Verlag.